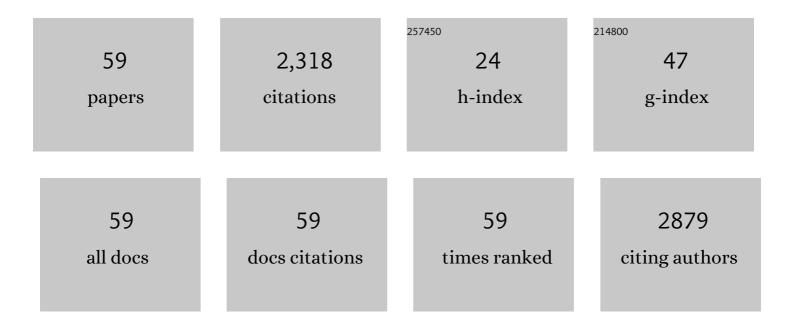
## Xiao-Fei Li

List of Publications by Year in descending order

Source: https://exaly.com/author-pdf/2802432/publications.pdf Version: 2024-02-01



XIAO-EFLL

#	Article	IF	CITATIONS
1	Conversion of Dinitrogen to Ammonia by FeN <sub>3</sub> -Embedded Graphene. Journal of the American Chemical Society, 2016, 138, 8706-8709.	13.7	562
2	Theoretical Investigation of Broadband and Wide-Angle Terahertz Metamaterial Absorber. IEEE Photonics Technology Letters, 2014, 26, 111-114.	2.5	176
3	Industrial wastes applications for alkalinity regulation in bauxite residue: A comprehensive review. Journal of Central South University, 2019, 26, 268-288.	3.0	114
4	Unraveling the formation mechanism of graphitic nitrogen-doping in thermally treated graphene with ammonia. Scientific Reports, 2016, 6, 23495.	3.3	111
5	Effect of length and size of heterojunction on the transport properties of carbon-nanotube devices. Applied Physics Letters, 2007, 91, 133511.	3.3	109
6	Cooperative Spin Transition of Monodispersed FeN <sub>3</sub> Sites within Graphene Induced by CO Adsorption. Journal of the American Chemical Society, 2018, 140, 15149-15152.	13.7	108
7	Frequency Continuous Tunable Terahertz Metamaterial Absorber. Journal of Lightwave Technology, 2014, 32, 1183-1189.	4.6	102
8	A simple design of ultra-broadband and polarization insensitive terahertz metamaterial absorber. Applied Physics A: Materials Science and Processing, 2014, 115, 1187-1192.	2.3	67
9	SiC/MoS2 layered heterostructures: Promising photocatalysts revealed by a first-principles study. Materials Chemistry and Physics, 2018, 216, 64-71.	4.0	63
10	Big Bandgap in Highly Reduced Graphene Oxides. Journal of Physical Chemistry C, 2013, 117, 6049-6054.	3.1	52
11	Design of Graphene-Nanoribbon Heterojunctions from First Principles. Journal of Physical Chemistry C, 2011, 115, 12616-12624.	3.1	49
12	Metamaterial-Based Low-Conductivity Alloy Perfect Absorber. Journal of Lightwave Technology, 2014, 32, 2293-2298.	4.6	49
13	A simple design of a broadband, polarization-insensitive, and low-conductivity alloy metamaterial absorber. Applied Physics Express, 2014, 7, 082601.	2.4	40
14	Leaching optimization and dissolution behavior of alkaline anions in bauxite residue. Transactions of Nonferrous Metals Society of China, 2018, 28, 1248-1255.	4.2	39
15	Migration and distribution of saline ions in bauxite residue during water leaching. Transactions of Nonferrous Metals Society of China, 2018, 28, 534-541.	4.2	37
16	Improving the Oxygen Reduction Reaction Activity of FeN <sub>4</sub> –Graphene via Tuning Electronic Characteristics. ACS Applied Energy Materials, 2019, 2, 6634-6641.	5.1	37
17	Rationally designed 2D/2D SiC/g-C <sub>3</sub> N <sub>4</sub> photocatalysts for hydrogen production. Catalysis Science and Technology, 2019, 9, 3896-3906.	4.1	35
18	Tunable bandwidth of the terahertz metamaterial absorber. Optics Communications, 2014, 325, 78-83.	2.1	33

Χιάο-Γει Li

#	Article	IF	CITATIONS
19	Half-filled energy bands induced negative differential resistance in nitrogen-doped graphene. Nanoscale, 2015, 7, 4156-4162.	5.6	32
20	Insights into enhanced visible-light photocatalytic activity of C <sub>60</sub> modified g-C <sub>3</sub> N <sub>4</sub> hybrids: the role of nitrogen. Physical Chemistry Chemical Physics, 2016, 18, 33094-33102.	2.8	31
21	Electric-field-induced widely tunable direct and indirect band gaps in hBN/MoS <sub>2</sub> van der Waals heterostructures. Journal of Materials Chemistry C, 2017, 5, 4426-4434.	5.5	29
22	Firstâ€principles study of magnetic properties in Agâ€doped SnO <sub>2</sub> . Physica Status Solidi (B): Basic Research, 2011, 248, 1961-1966.	1.5	26
23	Effect of intertube interaction on the transport properties of a carbon double-nanotube device. Journal of Applied Physics, 2007, 101, 064514.	2.5	25
24	Effect of ammonium chloride on leaching behavior of alkaline anion and sodium ion in bauxite residue. Transactions of Nonferrous Metals Society of China, 2018, 28, 2125-2134.	4.2	25
25	A simple nested metamaterial structure with enhanced bandwidth performance. Optics Communications, 2013, 303, 13-14.	2.1	23
26	Coupling effect on the electronic transport through dimolecular junctions. Physics Letters, Section A: General, Atomic and Solid State Physics, 2007, 365, 489-494.	2.1	22
27	Strong current polarization and perfect negative differential resistance in few-FeN <sub>4</sub> -embedded zigzag graphene nanoribbons. Physical Chemistry Chemical Physics, 2017, 19, 2674-2678.	2.8	19
28	Electronic transport through zigzag/armchair graphene nanoribbon heterojunctions. Journal of Physics Condensed Matter, 2012, 24, 095801.	1.8	18
29	A triangular shaped channel MIM waveguide filter. Journal of Modern Optics, 2012, 59, 1686-1689.	1.3	18
30	First principles study on magnetic properties in ZnS doped with palladium. European Physical Journal B, 2013, 86, 1.	1.5	18
31	Tunable Electronic and Magnetic Properties of Grapheneâ€Embedded Transition Metalâ€N <sub>4</sub> Complexes: Insight From Firstâ€Principles Calculations. Chemistry - an Asian Journal, 2018, 13, 3239-3245.	3.3	18
32	Family-dependent magnetism in atomic boron adsorbed armchair graphene nanoribbons. Journal of Materials Chemistry C, 2019, 7, 6241-6245.	5.5	16
33	Strong current polarization and negative differential resistance in chiral graphene nanoribbons with reconstructed (2,1)-edges. Applied Physics Letters, 2012, 101, 073101.	3.3	15
34	Spin Polarization-Induced Facile Dioxygen Activation in Boron-Doped Graphitic Carbon Nitride. ACS Applied Materials & Interfaces, 2020, 12, 52741-52748.	8.0	15
35	Nanomechanically induced molecular conductance switch. Applied Physics Letters, 2009, 95, 232118.	3.3	14
36	Realizing Fano-like resonance in a one terminal closed T-shaped waveguide. European Physical Journal B, 2015, 88, 1.	1.5	14

Xiao-Fei Li

#	Article	IF	CITATIONS
37	A broadband, polarisation-insensitive and wide-angle coplanar terahertz metamaterial absorber. European Physical Journal B, 2014, 87, 1.	1.5	13
38	Uniform and perfectly linear current–voltage characteristics of nitrogen-doped armchair graphene nanoribbons for nanowires. Physical Chemistry Chemical Physics, 2017, 19, 44-48.	2.8	13
39	Semiconductor to metal transition by tuning the location of N2AA in armchair graphene nanoribbons. Journal of Applied Physics, 2014, 115, 053707.	2.5	12
40	Realistic-contact-induced enhancement of rectifying in carbon-nanotube/graphene-nanoribbon junctions. Applied Physics Letters, 2014, 104, 103107.	3.3	12
41	Important Structural Factors Controlling the Conductance of DNA Pairs in Molecular Junctions. Journal of Physical Chemistry C, 2010, 114, 14240-14242.	3.1	11
42	Effects of Interface Roughness on Electronic Transport Properties of Nanotubeâ^'Moleculeâ^'Nanotube Junctions. Journal of Physical Chemistry C, 2010, 114, 12335-12340.	3.1	11
43	Alkalinity stabilization behavior of bauxite residue: Ca-driving regulation characteristics of gypsum. Journal of Central South University, 2019, 26, 383-392.	3.0	11
44	Tuning the Electronic Transport Properties of Zigzag Graphene Nanoribbons via Hydrogenation Separators. Journal of Physical Chemistry C, 2011, 115, 24366-24372.	3.1	10
45	Ferromagnetic coupling in Mgâ€doped passivated AlN nanowires: A firstâ€principles study. Physica Status Solidi (B): Basic Research, 2012, 249, 185-189.	1.5	10
46	Tuning electronic and magnetic properties of armchair zigzag hybrid graphene nanoribbons by the choice of supercell model of grain boundaries. Journal of Applied Physics, 2014, 115, 104303.	2.5	10
47	Interface Magnetism in Topological Armchair/Cove-Edged Graphene Nanoribbons. Journal of Physical Chemistry C, 2020, 124, 15448-15453.	3.1	9
48	Conductivity of carbon-based molecular junctions from ab-initio methods. Frontiers of Physics, 2014, 9, 748-759.	5.0	5
49	Tuning electron transport through a single molecular junction by bridge modification. Journal of Applied Physics, 2014, 116, .	2.5	5
50	Isolated pentagons induced enhancement of conductance in ultra-narrow armchair graphene nanoribbon junctions. Journal of Applied Physics, 2016, 120, 164303.	2.5	5
51	Resonance induced spin-selective transport behavior in carbon nanoribbon/nanotube/nanoribbon heterojunctions. Physics Letters, Section A: General, Atomic and Solid State Physics, 2015, 379, 1722-1725.	2.1	4
52	Ultrahigh conductivity of graphene nanoribbons doped with ordered nitrogen. Nanoscale Advances, 2019, 1, 4359-4364.	4.6	4
53	Strong current-polarization and negative differential resistance in FeN3-embedded armchair graphene nanoribbons. Chinese Journal of Chemical Physics, 2018, 31, 756-760.	1.3	4
54	Superlight and Superflexible Threeâ€Đimensional Semiconductor Frameworks A(X≡Y) <sub>4</sub> (A=Si,) 1	īj ETQq0 0 3.3	0 rgBT /Overl 3

. Chemistry - an Asian Journal, 2017, 12, 804-810.

		Χιλο-Γει Li		
#	Article		IF	CITATIONS
55	Perfect spin-filtering in p-aminophenol functionalized zigzag graphene nanoribbons: The hybridized nitrogen. Physics Letters, Section A: General, Atomic and Solid State Physics, 2093-2096.	e role of sp3 , 2019, 383,	2.1	2
56	Folded C-Type SIW Butler Matrix. , 2019, , .			1
57	Rectification with controllable directions in sulfur-doped armchair graphene nanoribbon heterojunctions. Chemical Physics, 2021, 546, 111140.		1.9	1
58	A 4×4 Planar Dual-Polarization Retrodirective Array. , 2021, , .			1
59	First-Principles Observation of Bonded 2D B4C3 Bilayers. ACS Omega, 2021, 6, 13218-1	13224.	3.5	0